https://doi.org/10.5194/egusphere-2026-2026
Preprint. Discussion started: 27 April 2026

Interaction between the East Asian summer monsoon and Westerlies as shown by desert shrub-ring records from the Alxa Plateau, Northwest China

Shengchun Xiao[1]*, Xiaomei Peng[1], Aijun Ding[2], Quanyan Tian[1], Yu Ren[1,3]，Jiakang Wang[1,3]

[1] Northwest Institute of Eco-Environment and Resources, Chinese Academy of Sciences, Lanzhou, Gansu, China 730000.

[2] College of Resources and Environment, Gansu Agricultural University, Lanzhou, Gansu, China 730070.

[3] University of Chinese Academy of Sciences, Beijing, China 100049.

* Corresponding author: Shengchun Xiao (xiaosc@lzb.ac.cn).

Address: 320 West Donggang Road, Lanzhou City, Gansu Province, China.

Zip Code: 730000.

https://doi.org/10.5194/egusphere-2026-2026
Preprint. Discussion started: 27 April 2026

Abstract:

The variations, driving mechanisms, and interactions between the mid-latitude westerlies and the Asian summer monsoon represent a critical focus in global change research. Extensive research has investigated climate change and its drivers across multiple timescales in the core regions of both westerlies Asia and monsoonal Asia. However, studies are far fewer in the arid inland deserts at the interactive margin of these two circulation systems, where precipitation restrict the distribution of trees. To address this gap, we developed 26 shrub-ring width chronologies of *Zygophyllum xanthoxylum* from four sub-regions of the Alxa Desert Plateau. Our analysis reveals that shrub radial growth is primarily limited by aridity during the growing season, driven by low precipitation. The four regional chronologies indicate substantial spatiotemporal heterogeneity in dry–wet variability. By integrating these records with indices of the westerlies and the East Asian summer monsoon (EASM), we demonstrate that hydroclimatic variations are primarily modulated by the interaction between these two circulations. The Alxa Plateau is predominantly influenced by the EASM, whose boundary can extend approximately 400 km northwestward to the Yabulai–Nurgong–Lang mountains line in the central plateau. This can cover the entire Tengger and Ulan Buh Deserts. Concurrently, the westerlies can advance eastward to affect the Helan Mountains. Thus, the Alxa Plateau constitutes a key transition zone and interaction arena between the westerlies and the EASM within China's arid interior. At the same time, the foehn effect in the mountains around the Alxa Plateau also has a certain impact on atmospheric circulation. Climatic fluctuations in this region critically influence local vegetation dynamics and desertification processes, underscoring its importance for understanding past and future environmental change.

Key words: Alxa Plateau; Shrub-dendroclimatology; Interaction between Westerlies and East Asian summer monsoon; *Zygophyllum xanthoxylum*.

https://doi.org/10.5194/egusphere-2026-2026
Preprint. Discussion started: 27 April 2026

1. Introduction

Two atmospheric circulation systems, the mid-latitude Westerlies and the Asian summer monsoon, play key roles in the northern hemisphere climatic changes (An et al., 2012). The eastern part of the arid and semi-arid region of Central and East Asia lies on the margin of the East Asian monsoon domain and is influenced by both the westerly and monsoon circulations (Wang, 2006; Liu et al., 2018) (Figure 1). From the perspective of large-scale atmospheric systems, Chen et al. (2009) divided the Asian continent into two major climatic domains: the "Westerlies Asia", primarily controlled by the mid-latitude westerlies, and the "Monsoonal Asia", primarily governed by the monsoon circulation.

The arid northwestern China, located in the interior of the Eurasian continent, is one of the driest areas globally at the same latitude. It exhibits the typical characteristics of a continental climate, with a westerly circulation pattern. While primarily influenced by the westerlies, this region is also affected by the East Asian monsoon. Precipitation decreases progressively from the eastern and western edges towards the central arid and semi-arid zone of Eurasia, accompanied by high variability and frequent droughts. Consequently, this area is considered both sensitive to and ecologically vulnerable to global climate change (Chen et al., 2019a; 2019b; Zhang et al., 2023).

The East Asian summer monsoon (EASM) is a circulation system that creates distinct differences in moisture levels (Tang et al., 2006a; Tang et al., 2006b). The fluctuating northern boundary of the monsoon is known as the northern marginal zone (Xu and Qian, 2003; Hu and Qian, 2007). According to Chen et al. (2018), the 300 mm isohyet is used as a climatic indicator to define the northern boundary of the EASM in China. In northwestern China, this climatic boundary roughly coincides with the Qilian, Helan and Daqing mountains.

The westerly zone is a vital link between the North Atlantic climatic region and the East Asian monsoon region (Qu et al., 2004). Variations in the westerlies directly affect moisture transport; a significant amount of the moisture in northwestern China in summer originates from the interaction between the westerlies and the monsoon (Feng et al., 2004; Wang et al., 2005; Li et al., 2008; Ma et al., 2011; Luo et al., 2026). Moreover, dust storm activity in northern China is closely linked to changes in the location and strength of the mid-latitude westerly jet (Zhong and Li, 2005; Li and Liu, 2015).

https://doi.org/10.5194/egusphere-2026-2026
Preprint. Discussion started: 27 April 2026

Against the background of global atmospheric circulation changes, the advance, retreat, positional shifts, and interactions of the EASM and westerly circulation are inevitably affected. These changes further influence climate variability in northwestern China, consequently affecting ecological and environmental dynamics. Research on the climate and environment in this region is of significant theoretical and practical importance, making it a key issue in global change studies (Chen et al., 2019a; Chen et al., 2019b).

Dendroclimatology provides high-resolution, annually resolved proxy data on centennial to millennial scales, which are invaluable for reconstructing monsoon and westerly circulation histories, and for investigating the driving mechanisms of climate change (Liu et al., 2001; Liu and Cai, 2003; Liu et al., 2008; Chen et al., 2013; Kang and Yang, 2015). However, previous research has predominantly focused on the core zones influenced by the westerlies or the monsoon. In these regions, dendroclimatic studies and investigations into climate forcing mechanisms have largely been based on individual sampling sites. There remains a scarcity of comprehensive, multi-site, and regional-scale research that systematically examines the linkages with these major circulation systems. This gap is particularly pronounced in the transition zone where the westerlies and the East Asian summer monsoon interact (Xiao et al., 2024a;b).

Xiao et al. (2024a) conducted a preliminary investigation into the interaction mechanisms between the EASM and the westerlies, using tree-ring data from *Picea crassifolia* at three sites in the mountainous areas surrounding the arid Alxa Plateau in northwestern China. However, research on the core interaction zone between these two circulation systems—the interior desert region of the Alxa Plateau—remains notably scarce. This is largely because aridity limits the distribution of tree species across the plateau, meaning that dendroclimatology studies here are primarily based on shrubs.

This study uses tree-ring width chronologies from 26 *Zygophyllum xanthoxylum* sampling sites, a dominant shrub species in the Alxa Plateau desert ecosystem, to analyze the climatic response characteristics of its radial growth across four distinct regions. By integrating the Westerly and EASM indices, we further investigate how these two major circulation systems and their interactions drive regional climate variability. The study aims to clarify the spatiotemporal heterogeneity of climate change in the desert and the surrounding mountains of

https://doi.org/10.5194/egusphere-2026-2026
Preprint. Discussion started: 27 April 2026

Alxa Desert Plateau, and to elucidate the interaction mechanisms between the two circulation systems. This will provide a theoretical basis for climate change research and desertification control in arid regions.

2. Study area, Material and methods

2.1 Study area

The Alxa Plateau is located to the north of the Hexi Corridor in China's Gansu Province, and west of the Inner Mongolia Plateau，and south of the Gobi Altai Mountain (Figure 1). Three deserts distribute in this area, including of the Tengger Desert, the Ulan Buh Desert, and the Badain Jaran Desert. Several mountain ranges surround and span the Alxa Plateau. These include the Helan Mountains to the east, the northern mountains of the Hexi Corridor to the south, the outliers of the Altai Mountains to the north, and a series of denuded lower mountain ranges of the Yabulai, Nurgong, Zongnai and Lang mountains in the middle. These mountains not only block the desert's eastward and southward expansion (driven by high-pressure regions from Mongolia), but also form the headwaters for rivers and streams that water the oases on the plateau (Xiao et al. 2024a) (Figure 1).

The Alxa Plateau is located in the eastern margin of the inland, arid region of Central Asia. Many studies showed that this area is the main interaction zone of the mid-latitude westerly circulation and the Asian monsoon (Xiao et al., 2017; Chen et al., 2019b; Xiao et al., 2024a;b). Its pronounced interannual variability effects on the vegetation cover changes (Ou and Qian, 2006; Tang et al., 2006a; 2006b; Li et al., 2013; Ren et al. 2026).

The Alxa Plateau has a typical continental climate. We have divided the study area into four regions based on geographical distribution characteristics of the three major deserts and the sampling points (Figure 1): the Yabulai-Nurgong low mountain area (RN), the Ulan Buh Desert area (RW), the Badain Jaran Desert area (RY), and the Tengger Desert area (RT).

https://doi.org/10.5194/egusphere-2026-2026
Preprint. Discussion started: 27 April 2026

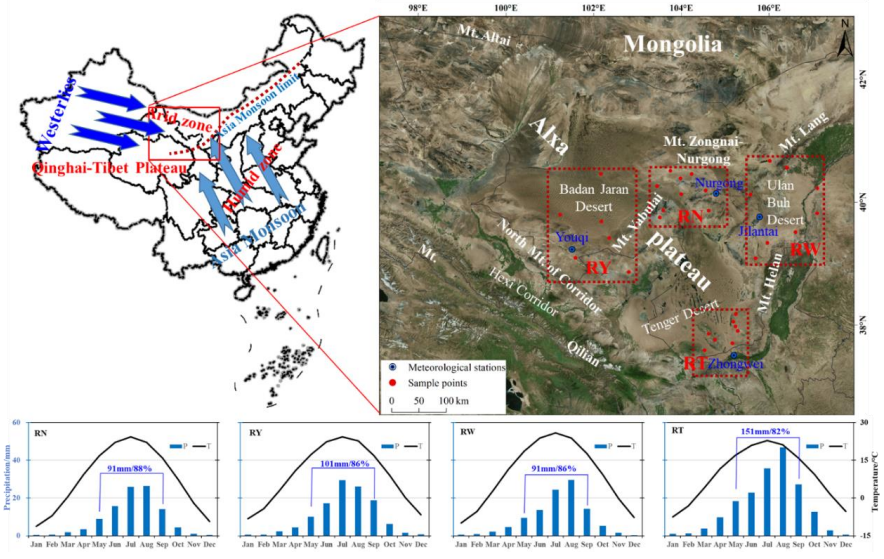

Figure 1. Location of tree-ring sampling sites（red points）and a climatic diagram (1955－2017) of the study area in RY (Youqi meteorological station,1960-2017), RN (Nurgong meteorological station,1957-2017), RW (Jilantai meteorological station,1955-2017) and RT(Zhongwei meteorological station,1959-2017). The blue box and appended data in the climatic diagram indicate the total growing season (from May to September) precipitation in the study area and the proportion of total annual precipitation. The red dashed boxes indicate the four regions in the study area. This figure is modified after Xiao et al. (2024a).

Meteorological data for the study regions RN, RY, RW, and RT were obtained from the nearest stations at Nurgong, Youqi, Jilantai, and Zhongwei, respectively. The annual mean temperatures at these stations are 7.4 ℃, 8.9 ℃, 8.8 ℃, and 9.0 ℃, respectively (http://data.cma.cn). The multi-year average annual precipitation is 103.0 mm, 118.0 mm, 106.9 mm, and 182.9 mm, respectively. Notably, 82－88% of the precipitation concentrated from May to September (Figure 1).

Z. xanthoxylum is a super-xerophilous and soil-stabilizing species endemic to Central Asia's deserts, and often serves as a dominant or constructive species in the gravelly riparian terraces, gently sloping hills, and pre-hill flood fans in the Alxa Desert (Xiao et al., 2012; Chen et al., 2016). *Z. xanthoxylum* has well-defined annual growth rings, making it suitable for tree-ring study (Xiao et al., 2019; Ding et al., 2021). Recently, shrub-ring data of this species have

https://doi.org/10.5194/egusphere-2026-2026
Preprint. Discussion started: 27 April 2026

been used to conduct climate reconstruction and ecological response studies in the Badain Jaran, Tengger and Ulan Buh deserts, providing a new perspective for studying climate and environmental changes in arid regions (Xiao et al., 2012; Xiao et al., 2019; Ding et al., 2021; Peng et al., 2024; Ding et al., 2025).

2.2 Data collection, processing, and analysis

2.2.1 Sample collection, processing, and chronology construction

A total of 26 sampling sites of the shrub *Z. xanthoxylum* were collected from the Alxa Plateau between 2007 and 2024 (Figure 1). The Supplementary Table 1 (S1) provides detailed information on the location, sample size, chronology length of ring width, mean sensitivity, credible chronology interval with a subsample signal strength (SSS) >0.85, and signal-to-noise ratio for each chronology.

For each sampling sites, shrub disc treatment, cross-dating and ring width measurement were carried out according to the standard method of dendrochronology, and the standard chronologies was finally constructed（(Holmes, 1983; Cook, 1985; Xiao et al. 2019; Ding et al., 2025）。

A regional tree-ring chronology (Figure 2) was generated by calculating the weighted mean of the standardized chronology indices from all sample sites within the region. The weight for each site in a given year was determined by the proportion of its index value relative to the sum of the indices from all sites for that given year. This method of constructing the chronology can help enhance the strength of low-frequency signals to a certain extent.

2.2.2 Atmospheric circulation indices and correlation analysis

The East Asian summer monsoon index (EASMI defined by Li and Zeng (2005) for the period 1950–2017) and the westerly circulation index (WCI annual mean, period 1951–2015) (https://cmdp.ncc-cma.net/cn/index.htm) were same as Xiao et al.(2024a).

Response-function analysis was used to quantify the relationships between tree-ring chronologies and climate variables, using the DENDROCLIM2002 software (Biondi and Waikul, 2004). The climate variables included the total monthly precipitation, mean monthly temperature measured at the nearest meteorological station in study area (Figure 1), and the standardized precipitation evapotranspiration index (SPEI) over a 13-month period (from

https://doi.org/10.5194/egusphere-2026-2026
Preprint. Discussion started: 27 April 2026

September of the previous year to September of the current year). The SPEI was calculated based on observational data, using the SPEI package (https://CRAN.R-project.org/package=SPEI) in R software, and used the FAO-56 Penman-Monteith equation for potential evapotranspiration (Beguería et al., 2014).

Interannual and interdecadal (sliding moving average of 11 years) chrono-climatic and chrono-cyclonic indices correlation and partial correlation analyses were performed using SPSS 19.0. Based on the characteristics of the two circulation indices, the sequences were classified into three groups (low, medium, and high) using the mean ±1 standard deviation as the threshold. Correlation tests were conducted between these three grouped circulation indices and the corresponding tree-ring indices.

3. Results and analysis

3.1 Regional chronologies and climate response characteristics

Regional chronologies exhibit high spatial heterogeneity in interannual variability (Figure 2). At the decadal scale (11-year moving average), consistent changes are evident in the four regional chronologies around the 1890s, late 1910s to late 1950s, and late 1980s to late 2000s. The period from late 1910s to late 1950s represents a low-growth phase, while the other two periods correspond to consistent high-growth phases.

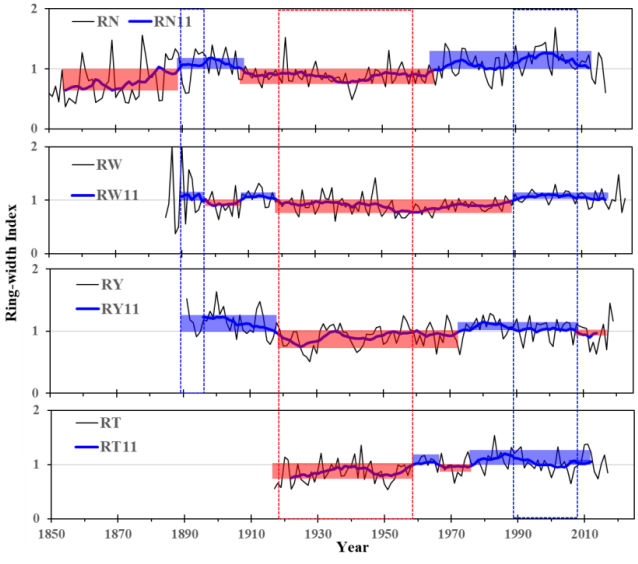

Figure 2. Spatial heterogeneity of *Z. xanthoxylum* radial growth in the Alxa Desert.

https://doi.org/10.5194/egusphere-2026-2026
Preprint. Discussion started: 27 April 2026

Note: Red bands denote periods of reduced growth in the 11-year moving average chronology, while blue bands indicate periods of enhanced growth. Red dashed boxes highlight intervals of reduced growth that show multi-regional agreement across the chronologies, while blue dashed boxes mark periods of enhanced growth with similar multi-regional consistency.

Correlation analysis between the four regional chronologies and the climate variables reveals spatially heterogeneous correlation patterns. The climate variables include monthly mean temperature, monthly precipitation, and SPEI at different scales (1962–2017). Correlation analysis of SPEI across scales from 1 to 12 months revealed the greatest significance at the 9-month scale (Figure 3).

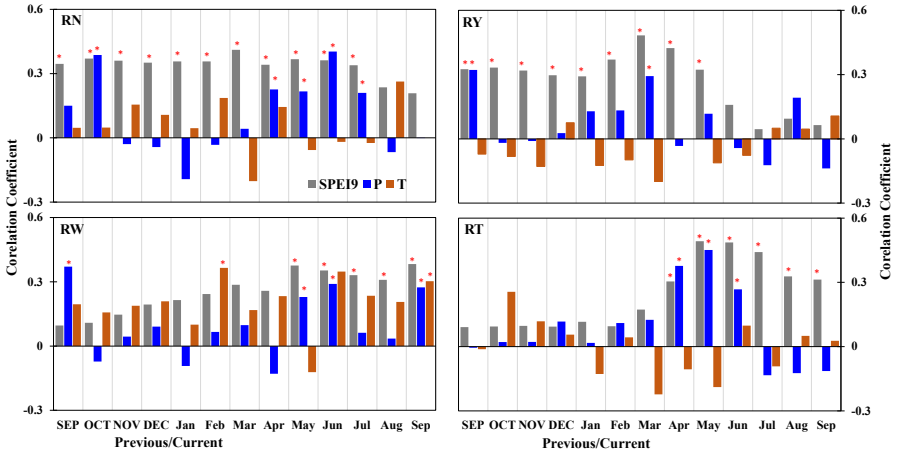

Figure 3. Correlation between the four regional chronologies and monthly mean temperature (red), monthly precipitation (blue), and 9-month scale SPEI (grey). * Pearson's r correlation, significant at $P < 0.05$.

Overall, the four regional chronologies exhibit a positive correlation with the SPEI from September of the previous year to September of the current year, always achieving significant levels in the growing season. The four regional chronologies also significantly correlate with the average 9-month scale SPEI from April to August. A predominantly positive correlation was observed between the four regional chronologies and monthly precipitation during the growing season, reaching significant levels, particularly in the RN, RW, and RT, from April to June, with most months achieving significance levels. A significant positive correlation with monthly mean temperature was evident in the RW in February and September of the current year, while

https://doi.org/10.5194/egusphere-2026-2026
Preprint. Discussion started: 27 April 2026

the other three chronologies exhibited weak negative correlations with monthly mean temperatures during the growing season.

These findings indicate that radial growth variation of *Z. xanthoxylum* on the Alxa Desert Plateau is primarily constrained by climatic aridity, resulting from low precipitation during the growing season.

3.2 Interannual and decadal characteristics of the influence of two circulation systems on the radial growth of desert shrubs

To investigate the impact of two major circulation systems on the radial growth of desert shrubs on the Alxa Plateau, correlation analyses were conducted at the interannual scale, using the entire regional chronology and grouped circulation indices.

The results indicate that no significant correlations were observed among the four regional chronologies or their groupings at the interannual scale (Figure 4). Analysis of the two major circulation indices revealed relatively consistent correlations between the medium index group and the four regional chronology indices: negative with WCI, and positive with EASMI. The low WCI index group showed positive correlations with RN and RT, and negative correlations with RW and RY. The high WCI index group exhibited positive correlations with the four regional chronologies. The low EASMI index group exhibited negative correlations with the four regional chronologies. For the high EASMI index group, negative correlations were observed with all four regional chronologies, except RT.

Overall, shrub diameter growth in the medium index group showed a negative correlation with WCI, and a positive correlation with EASMI. For the high and low index groups, however, shrub growth showed inconsistent correlations with WCI and EASMI.

Correlation analysis between the two circulation indices and the four regional chronologies at the interdecadal scale (Figure 5) indicates a negative correlation between the four chronologies and the EASMI ($p < 0.01$), especially in the Ulan Buh Desert and the Nurgong mountain. For the WCI, the Ulan Buh Desert (RW) and Nurgong (RN) regions showed a significant positive correlation. Conversely, the Tengger Desert (RT) and Badain Jaran Desert (RY) showed insignificant negative correlations.

https://doi.org/10.5194/egusphere-2026-2026
Preprint. Discussion started: 27 April 2026

Further partial correlation analysis of the two circulation indices and four regional chronologies at the decadal scale revealed that all four chronologies exhibited significantly negative correlations with EASMI when controlling for the WCI variable. Controlling for the EASMI variable produced significant positive correlations between the RN and RW in the northern Alxa Plateau and the WCI, while the RY and RT in the southern Alxa Plateau showed negative correlations, with only the RY reaching statistical significance (see Table 1).

As shown in Figure 5, the WCI exhibits four discernible phases on a decadal scale: a gradual strengthening phase (1956–1963), followed by a weakening phase (1964–1979), a renewed strengthening period (1980–1994), and a subsequent weakening phase (1995–2011). The highest index values occurred primarily during two intervals: 1962–1967 and 1989–2007. In contrast, the lowest values were observed between 1971–1985 and 1956–1958.

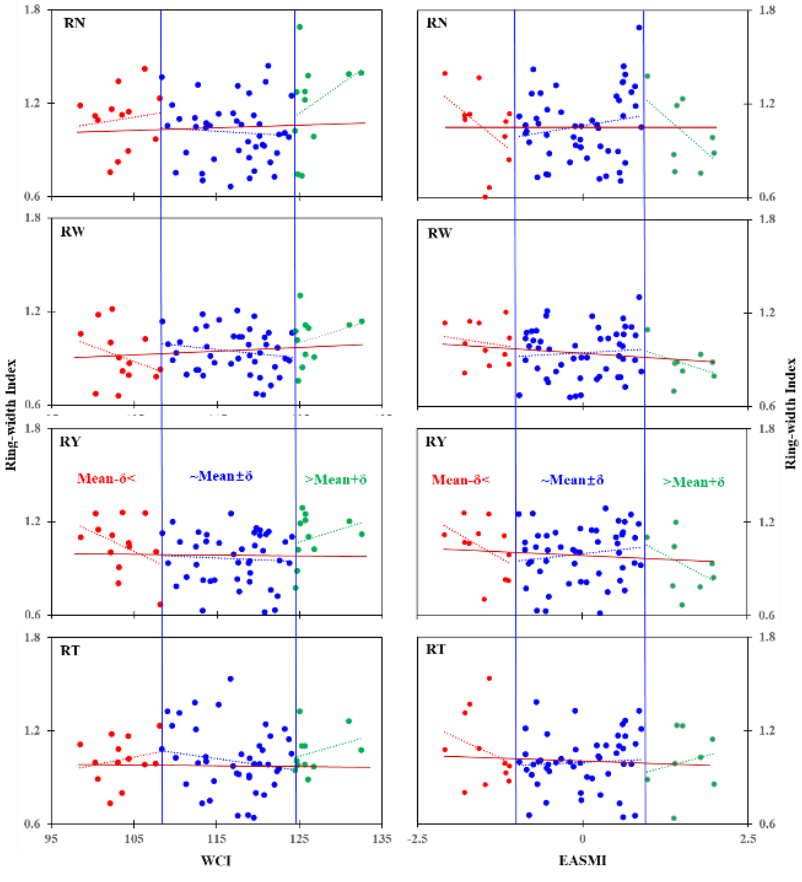

Figure 4. Correlation between the *Z. xanthoxylum* radial growth and the East Asian summer

https://doi.org/10.5194/egusphere-2026-2026
Preprint. Discussion started: 27 April 2026

monsoon index (EASMI) and Westerlies Index (WCI).

Note: Linear fits between the chronologies and circulation indices are shown for the whole series (red solid line) and for low, medium, and high index groups (red, blue, and green dashed lines, respectively). None of these fits were significant ($p > 0.05$).

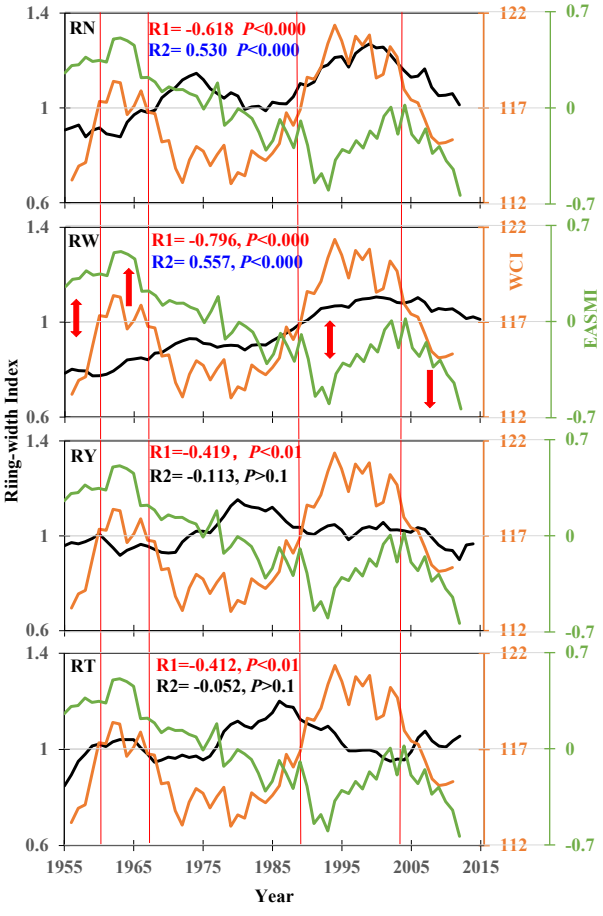

Figure 5. Correlations between the four regional chronologies (black) on the Alxa Plateau and the EASMI (green) and WCI (brown) at the decadal scale (11-year moving average), alongside features of their interaction. R1 and R2 represent the respective correlation coefficients and significance levels between the chronologies and EASMI/WCI. Red arrows indicate periods when both circulation systems were typically strong (upward), weak (downward), or when one was strong and the other was weak (bidirectional).

https://doi.org/10.5194/egusphere-2026-2026
Preprint. Discussion started: 27 April 2026

The EASMI exhibited a strengthening phase from 1955 to 1963, followed by a weakening phase from 1964 to 1993, another strengthening phase from 1994 to 1982, and then a weakening phase from 1983 to 2011. During the entire study period, the strongest EASMI occurred from 1955 to 1978, while the weakest values were observed from 1990 to 1998 and from 2011 to 2012.

Table 1. Partial correlation analysis of the regional chronologies on the Alxa Plateau with the EASMI and WCI

Control variables	RN	RW	RY	RT
WCI	-0.609***	-0.794***	-0.469***	-0.432***
EASMI	0.458***	0.545***	-0.274*	-0.198

Note: Two-tailed correlation test (n=53): ***($p < 0.001$), *($p < 0.05$);

Four patterns can be identified based on the intensity characteristics of the two circulation systems over the decadal scale: both circulations are strong (e.g., 1960–1966); both circulations are weak (e.g., 1980–1988 and 2005–2015); the WCI is strong and the EASMI is weak (e.g., 1990–1998); and the WCI is weak and the EASMI is strong (e.g., 1955–1959) (Figure 5).

When both circulation indices were strong, the chronology indices of the RN, RW, and RY were relatively low, while the RT indices were relatively high. Under the pattern of a strong WCI and weak EASMI, the chronology indices of the RN and RW were relatively high, while those of the RY and RT were relatively low. When both circulation indices were weak, the values across the four chronologies were inconsistent. For example, during 1980–1988, the indices of the RN, RW, and RT showed an upward trend, whereas the RY exhibited a downward trend. Conversely, during 2005–2015, the indices in the RN, RW, and RY declined, while an upward trend was observed in the RT. When the WCI was weak and the EASMI was strong, the chronology indices in the RN, RW, and RT were relatively low, while the RY indices were close to the mean level.

The above results indicate that the radial growth of Z. xanthoxylum in different regions of the Alxa Plateau varies spatially in response to the interplay between the two circulation systems. When the EASMI is weak and the WCI is strong, radial growth is enhanced in the

https://doi.org/10.5194/egusphere-2026-2026
Preprint. Discussion started: 27 April 2026

northern parts of the plateau (RN and RW), but suppressed in the southern parts (RY and RT). Conversely, when the EASMI is strong and the WCI is weak, radial growth is generally inhibited across all four regions. When both circulation systems are strong, growth is favorable only in the RT region, and unfavorable in the other three regions. When both circulation systems are weak, radial growth is suppressed in the northern regions (RN and RW), but promoted in the southern regions (RY and RT).

Overall, the study area is predominantly influenced by the EASM. However, the Westerlies exert a significant impact on the central-southern, central-northern, and north-eastern parts of the Alxa Plateau, except in the south-eastern region (RT), where its influence is weaker. Consequently, we propose that the interaction zone between the EASM and the Westerlies is primarily located in the central and northern parts of the Alxa Plateau (see Figure 6). Furthermore, the northern boundary of the EASM extends approximately 400 km northwestwards to the Yabulai–Nurgong–Lang Mountains line, covering the entire Tengger and Ulan Buh deserts in the process. Meanwhile, the Westerlies can advance eastwards, influencing areas up to the Helan Mountains.

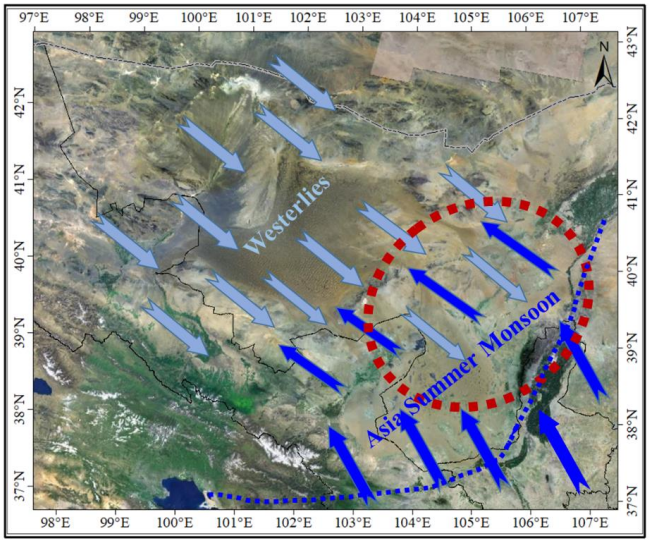

Figure 6. Schematic diagram showing the interaction between the EASM (dark blue arrows) and the Westerlies (light blue arrows) on the Alxa Plateau. The blue dashed lines show the

https://doi.org/10.5194/egusphere-2026-2026
Preprint. Discussion started: 27 April 2026

conventional EASM boundary, while the red circles highlight the primary area of interaction between the EASM and Westerlies. This figure is modified after Xiao et al. (2024a).

4. Discussion and Conclusions

4.1 Climate changes of deserts indicated by regional chronologies.

Similar to the findings of other dendroclimatic studies in arid and semi-arid regions (Xiao et al., 2012; Xiao et al., 2019; Xiao et al., 2024a; Ding et al., 2025), the radial growth of *Z. xanthoxylum* in the four regions of the Alxa Plateau is primarily limited by low precipitation and high temperatures. There is a significant positive correlation between radial growth and the growing-season drought index. Consequently, the four regional chronologies primarily reflect regional moisture variations (Figure 4).

On an interannual scale, the four regions exhibit coherent dry/wet patterns, as well as considerable spatiotemporal heterogeneity (Figure 2). Arid conditions dominate for a larger proportion of the time across the four regions. This is particularly evident in northern Alxa Plateau, where the longest continuous drought occurred from the 1910s to the 1980s, with the most severe drought happening during the 1850s–1860s. A relatively consistent humid phase occurred mainly from the late 1980s to the late 2000s across the four regions, though the timing, duration, and intensity of this phase varied between regions. These characteristics reflect the inherently arid nature of the inland desert climate.

On a broader (interdecadal) scale, an extreme drought period in the 1920s – 1930s was shared by much of northern China (Liang et al., 2006; Fang et al., 2009; Fang et al., 2010). On a decadal scale, a comparison of the four desert chronologies from the Alxa Plateau and three chronologies from the surrounding mountains (Xiao et al., 2024a) indicates that all of them experienced a sustained dry phase from the 1920s to the early 1930s (Figure 7). This drought event persisted for approximately half a century.

A humid phase during the 1990s–2000s was revealed by both the two northern chronologies of Alxa (RN and RW) and the chronologies from nearby Helan Mountains. This humid period lasted longer and was relatively more pronounced in the desert regions than in the mountains, especially in the northwestern Alxa (RN). The RN region also recorded a synchronous dry period with the Helan Mountains around the 1860s. In RN, this drought

https://doi.org/10.5194/egusphere-2026-2026
Preprint. Discussion started: 27 April 2026

342 persisted until the late 1880s, whereas in the Helan Mountains, it transitioned to a humid phase
343 in the mid-1860s, which continued until the mid-1880s (Figure 7). During the 1900s and 1980s,
344 the two southern chronologies from the Alxa Desert (RY and RT) indicated periods of increased
345 humidity, which coincided with the northern mountains of the Hexi Corridor (DS). Once again,
346 the desert regions exhibited higher moisture levels.

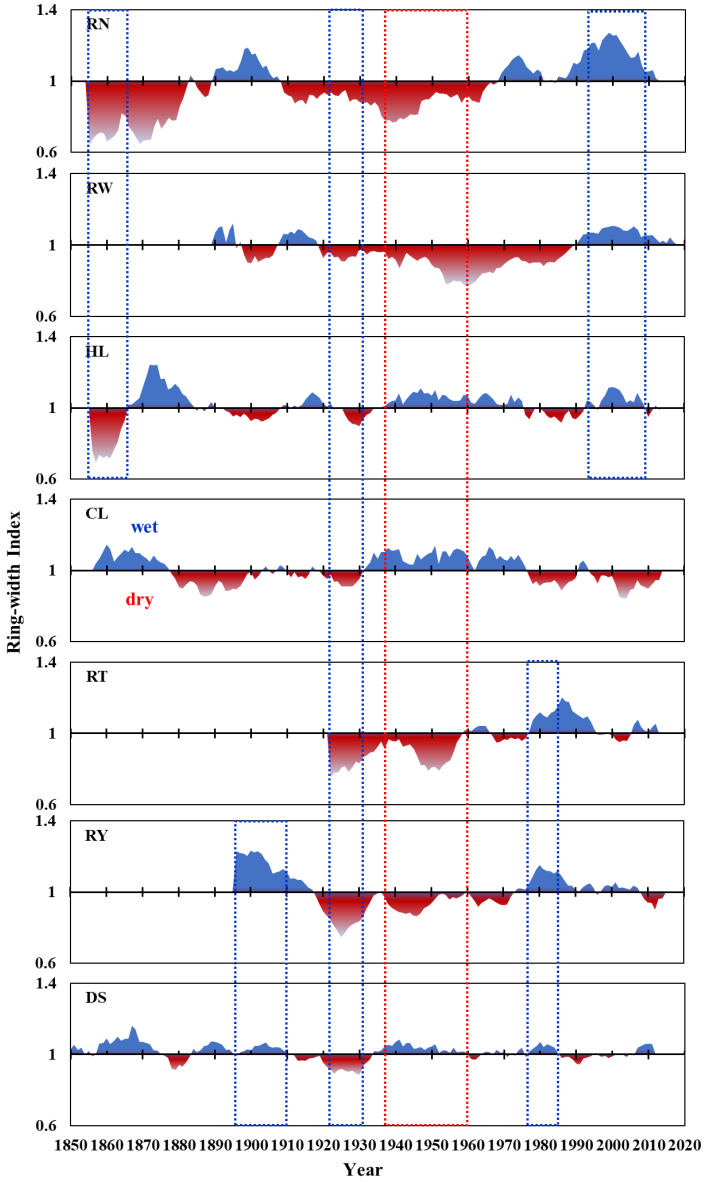

347

348 Figure 7. Comparison of wet/dry variations between the desert chronologies of the Alxa Plateau

https://doi.org/10.5194/egusphere-2026-2026
Preprint. Discussion started: 27 April 2026

(RN, RW, RY, RT) and tree-ring records from the surrounding mountains (HL: Helan Mountains; CL: Changling Mountains; DS: Dongda Mountains; data from Xiao et al., 2024a). Blue boxes denote periods of consistent moisture variation, while red boxes indicate opposing trends between the desert and mountain sites.

From the 1930s to the late 1950s, the Alxa Desert experienced a dry phase, while the surrounding mountains were in a humid phase, reflecting an opposite climatic tendency between the two types of terrain. This opposite climatic condition persisted for nearly half a century, or even longer, in this area. The dry periods captured in the desert chronologies are consistent with earlier single-site climate reconstructions (Xiao et al., 2012; Xiao et al., 2019; Ding et al., 2025). These humid periods were also documented in the monsoon-influenced mountainous areas east of the Alxa Plateau, as evidenced by local historical records (Yuan, 1994) and tree-ring chronologies from Mt. Xinglong (Fang et al., 2009; Chen et al., 2013) and Mt. Guiqing (Fang et al., 2010).

4.2 Influence of atmospheric circulations and their interaction on climate change in the Alxa Plateau

The westerly jet axis is situated near 40° N, and its zonal variation generates two pairs of cross-coupled positive and negative anomaly centers, one over the Iranian Plateau and the Mongolian Plateau, and the other over the Eastern Europe and Eastern China. The Alxa Plateau lies at the transitional margin between the Mongolian Plateau and Eastern China anomaly centers. Northward shifts of the westerly jet are generally associated with a slight increase in precipitation over the region, whereas southward shifts correspond to reduced precipitation (Sun et al., 2003; Guo et al., 2025).

When the westerlies intensify, their core shifts southwards, leading to increased precipitation in the central and northern parts of the Alxa Plateau. Conversely, a weakening of the westerlies results in reduced precipitation. At the same time, the cold, dry westerly airflow lowers regional temperatures, thereby reducing vegetation evapotranspiration and alleviating drought stress. Consequently, the radial growth of *Z. xanthoxylum* in the northern Alxa (RN and RW) shows a significant positive correlation with the WCI, whereas the two chronologies in

https://doi.org/10.5194/egusphere-2026-2026
Preprint. Discussion started: 27 April 2026

the southern Alxa (RY and RT) show a negative correlation (with RY reaching statistical significance) (Table 1). This finding is further supported by the significant positive correlation observed on a decadal scale between the WCI and the radial growth of *P. crassifoli*a in the Helan Mountains, east to the Alxa Plateau (Xiao et al., 2024a).

Research indicates that some of the moisture carried by the westerlies moves southwards after traversing northern Xinjiang, reaching northern Qinghai, the Hexi Corridor, northern Ningxia, and northern Shaanxi (Li et al., 2012). Western China lies within the zone of the prevailing westerlies, with the majority of moisture transported by these winds (Chen et al., 2008; 2009; 2010; Liu et al., 2017). Analyses indicate that the WCI is a reliable indicator of moisture transport and the moisture budget in northwestern China, primarily in summer. This is based on reanalysis data from the American National Environmental Protection Committee/National Center for Atmospheric Research (Feng et al., 2004; Wang et al., 2005; Li et al., 2008).

When the EASM intensifies, its warm, moist airflows are obstructed by high mountain ranges such as the Helan Mountains and the eastern Qilian Mountains at the monsoon boundary. This orographic lifting leads to precipitation on the windward side, while the descending air on the leeward side becomes warm and dry. This further exacerbates the high temperatures and aridity of the Alxa Plateau. Consequently, the radial growth of *Z. xanthoxylum* in the four regions of the plateau shows a significant negative correlation with the EASMI (Table 1). Dendroclimatological studies of *P. crassifolia* in the Helan and Changling Mountains, the southeastern part outside the Alxa, corroborate this mechanistic interpretation by reporting a positive correlation between radial growth and the EASMI on a decadal scale. This confirms the interception of warm, humid monsoon airflows by the surrounding mountains (Xiao et al., 2024a). This phenomenon is referred to as the foehn effect within a rain shadow area (where foehn refers to a type of dry, warm, and down-slope wind). Wind tunnel experiments and simulation indicate that the tropical semi-arid climate and the formation of desertified savanna in western Hainan Island, China, are primarily caused by the foehn effect associated with multiple mountain ranges in the rain shadow region (Li et al., 2006). Meteorological observations on both sides of the Southern Alps in New Zealand have also confirmed the occurrence of lee-side foehn effects resulting from orographic blocking (Mcgowan and Andrew,

https://doi.org/10.5194/egusphere-2026-2026
Preprint. Discussion started: 27 April 2026

1994). The Alxa Plateau is surrounded by high mountain ranges, including the Qilian Mountains, the North Mountains of the Hexi Corridor, the extensions of the Altai Mountains, and the Helan Mountains. These ranges have an average elevation of between 3,000 and 4,000 meters. These ranges block both major atmospheric circulation systems, creating significant foehn effects, which subsequently influence climate change and vegetation growth in the desert regions of the Alxa Plateau.

The southeastern Tengger Desert lies within a gap between the southern Helan Mountains and the eastern Qilian Mountains. This creates a topographic funnel effect that intensifies the interaction between the weakened edges of the two circulation systems. On a decadal scale, when the two circulation systems show contrasting intensities (one strong and one weak), *Z. xanthoxylum* radial growth in this region tends to be lower (Figure 5). Conversely, when both circulations are either strong or weak, radial growth tends to be higher. This pattern suggests that a more balanced state between the two circulation systems may reduce or counteract regional aridity, thereby favoring shrub growth. Decadal-scale correlation and partial correlation analyses further indicate that this area is primarily influenced by the EASM (Table 1).

A study of Holocene lake-level evolution in the ancient Zhuye Lake, on the central Alxa Plateau, showed that lake-level change was subject to the combined effects of EASM and the arid climate of Central Asia (Li, 2009). The radial growth of *Z. xanthoxylum* in the RY and RT is generally similar. However, due to its more westerly location, the RY is influenced by both the EASM and the Westerlies, as indicated by a significant partial correlation with the WCI (Table 1). Dendroclimatological studies from nearby mountains further illustrate this: on a decadal scale, the radial growth of *P. crassifolia* in the Changling Mountains (on the southern edge of the Tengger Desert) shows a positive correlation with the EASMI and a non-significant negative correlation with the WCI. In contrast, spruce growth in the Dongda Mountains (northern mountains of the Hexi Corridor, and southern edge of the Badain Jaran Desert) correlates positively with the EASMI, yet exhibits a significant negative correlation with the WCI (Xiao et al., 2024a).

Paleoclimate records from Qinghai Lake on the northern Tibetan Plateau indicate that the cold, dry Westerlies and the warm, humid EASM exhibited an anti-phase relationship on

https://doi.org/10.5194/egusphere-2026-2026
Preprint. Discussion started: 27 April 2026

glacial–interglacial to millennial scales during the late Quaternary. Another study of the nearby Toson Lake area also showed that the out-of-phase moisture transport and interaction between the Westerlies and EASM drive asynchronous lake evolution between Central and East Asia over centennial-millennial timescales (Li et al., 2022). Their interplay likely represented a dominant climatic mode in eastern Central Asia for much of this period (An et al., 2012). This anti-phase pattern is also evident in the instrumental indices of the two circulation systems over the past five decades (Figure 5). This interaction mechanism has also been confirmed by studies on the arid regions of Central Asia (Luo et al., 2026). These indices are constructed based on the seasonal to interannual positional shifts, boundary variations, and intensity changes of the atmospheric circulations (Zhang et al., 2003; Li and Zeng, 2005; Li et al., 2008; Chen and Chen, 2017; Chen et al., 2018). Consequently, the tree-ring chronologies from the four regions of the Alxa Plateau predominantly show inverse correlations with the two circulation indices on both interannual and decadal scales (Figure 5; Table 1).

Research using proxy indicator cycles has shown that the Alxa Plateau and its surroundings area are influenced by large-scale ocean-atmosphere oscillations on interannual and interdecadal scales, such as the North Atlantic Oscillation, Pacific Decadal Oscillation, El Niño-Southern Oscillation, and solar activity (Gou et al., 2015a; 2015b; Liu et al., 2016; Wang et al., 2017). The intensification of the EASM in humid monsoon regions and arid inland monsoon margins may be associated with rising temperatures in the Northern Hemisphere (An et al., 2012). However, all of the aforementioned large-scale climate and ocean-atmosphere changes affect the EASM and westerly circulation through different pathways (Li, 2009). These influences, in turn, have various effects on the northwestern margin of the EASM and the interaction zone between the two major atmospheric circulations, often with a lagged response (Ou and Qian, 2006). Consequently, over the past five decades, the phase relationship and interaction between the two circulations have exhibited additional strong-weak combinatorial patterns in response to global-scale climatic changes (Figure 5). This complexity has contributed to the heterogeneity of the spatiotemporal response of *Z. xanthoxylum* radial growth to climate across the four desert regions of the Alxa Plateau.

In conclusion, this dendroclimatological study, based on tree-ring width chronologies from 26 *Z. xanthoxylum* shrub sites across four desert regions of the Alxa Plateau (RN: Nurgong;

https://doi.org/10.5194/egusphere-2026-2026
Preprint. Discussion started: 27 April 2026

RW: Ulan Buh; RY: Badain Jaran; RT: Tengger), demonstrates that the radial growth of this desert shrub is primarily limited by drought conditions resulting from low precipitation during the growing-season. The dry/wet variations reflected in the four chronologies exhibit notable spatiotemporal heterogeneity, which is largely governed by the interaction between the EASM and Westerlies. While the entire study area is predominantly influenced by the EASM, and the northern and southwestern parts are also affected by the westerly jet. Consequently, the interaction between the westerly jet and the EASM occurs mainly over the central and northern Alxa Plateau, thereby driving regional vegetation dynamics and desertification processes.

Data availability. All data for this paper are available upon request.

Author contributions. All authors approved the manuscript and agreed on its submission. SX: conceptualization, methodology, funding acquisition, investigation, resources, writing (original draft, review and editing). XP: investigation, data collection and writing review. AD: investigation, data collection, and sample processing. QT: investigation. YR and JW: investigation and sample processing.

Competing interests. The contact author has declared that none of the authors has any competing interests.

Acknowledgments. This study was financially supported by the National Natural Science Foundation of China (Nos. 42171031) and Major Science and Technology Projects of the Inner Mongolia Autonomous Region (2024JBGS0009).

Disclaimer. Publisher's note: Copernicus Publications remains neutral with regard to jurisdictional claims made in the text, published maps, institutional affiliations, or any other geographical representation in this paper. While Copernicus Publications makes every effort to include appropriate place names, the final responsibility lies with the authors.

Review statement.

References

An, Z. S., Colman, S. M., Zhou, W. J., Li, X. Q., Brown, E. T., Jull, A. T., Cai, Y. J., Huang, Y. S., Lu, X. F., and Chang, H.: Interplay between the Westerlies and Asian monsoon recorded in Lake Qinghai sediments since 32 ka, Sci Rep, 2(1), 619, doi:https://doi.org/10.1038/srep00619, 2012.

https://doi.org/10.5194/egusphere-2026-2026
Preprint. Discussion started: 27 April 2026

499 Beguería, S., Vicente-Serrano, S. M., Reig, F., and Latorre, B.: Standardized precipitation
500 evapotranspiration index (SPEI) revisited: parameter fitting, evapotranspiration models,
501 tools, datasets and drought monitoring, Int. J. Climatol., 34(10), 3001–3023,
502 doi:https://doi.org/10.1002/joc.3887, 2014.
503 Biondi, F., and Waikul, K.: DENDROCLIM2002: A C++ program for statistical calibration of
504 climate signals in tree-ring chronologies, Comput. Geosci., 30(3), 303–311,
505 doi:https://doi.org/10.1016/j.cageo.2003.11.004, 2004.
506 Chen, F., Wei, W. S., Yuan, Y. J., Yu, S. L., Shang, H. M., Zhang, T. W., Zhang, R. B., Wang, H.
507 Q., and Qin, L.: Variation of annual precipitation during 1768-2006 in Gansu inferred from
508 multi-site tree-ring chronologies, Journal of Desert Research, 33(5), 1520, 2013.
509 Chen, F., Yuan, Y. J., Zhang, T. W., and Linderholm, H. W.: Annual precipitation variation for
510 the southern edge of the Gobi Desert (China) inferred from tree rings: linkages to climatic
511 warming of twentieth century, Nat. Hazards, 81(2), 939–955,
512 doi:https://doi.org/10.1007/s11069-015-2113-z, 2016.
513 Chen, F. H., Chen, J. H., Holmes, J., Boomer, I., Austin, P., Gates, J. B., Wang, N. L., Brooks,
514 S. J., and Zhang, J. W.: Moisture changes over the last millennium in arid central Asia: a
515 review, synthesis and comparison with monsoon region, Quat. Sci. Rev., 29(7-8), 1055–
516 1068, doi:https://doi.org/10.1016/j.quascirev.2010.01.005, 2010.
517 Chen, F. H., Chen, J. H., Huang, W., Chen, S. Q., Huang, X. Z., Jin, L. Y., Jia, J., Zhang, X. J.,
518 An, C. B., and Zhang, J. W.: Westerlies Asia and monsoonal Asia: Spatiotemporal
519 differences in climate change and possible mechanisms on decadal to sub-orbital
520 timescales, Earth-Sci. Rev., 192, 337–354,
521 doi:https://doi.org/10.1016/j.earscirev.2019.03.005, 2019a.
522 Chen, F. H., Fu, B. J., Xia, J., Wu, D., Wu, S. H., Zhang, Y. L., Sun, H., Liu, Y., Fang, X. M.,
523 and Qin, B. Q.: Major advances in studies of the physical geography and living
524 environment of China during the past 70 years and future prospects, Sci. China Earth Sci.,
525 49(11), 1659–1696, doi:https://doi.org/10.1007/s11430-019-9522-7, 2019b.
526 Chen, F. H., Sun, J. H., and Huang, W.: A discussion on the westerly-dominated climate model
527 in mid-latitude Asia during the modern interglacial period, Earth Sci. Front., 16(6), 23–32,
528 2009.

https://doi.org/10.5194/egusphere-2026-2026
Preprint. Discussion started: 27 April 2026

529 Chen, F. H., Yu, Z. C., Yang, M. L., Ito, E., Wang, S. M., Madsen, D. B., Huang, X. Z., Zhao,
530 Y., Sato, T., and Birks, H. J. B.: Holocene moisture evolution in arid central Asia and its
531 out-of-phase relationship with Asian monsoon history, Quat. Sci. Rev., 27(3-4), 351–364,
532 doi:https://doi.org/10.1016/j.quascirev.2007.10.017, 2008.
533 Chen, H. S., and Chen, J. K.: Classification of East Asian summer monsoon indices and their
534 basic physical features, Transactions of Atmospheric Sciences, 40(3), 299–309,
535 doi:https://doi.org/10.13878/j.cnki.dqkxxb.20160323001, 2017.
536 Chen, J., Huang, W., Jin, L. Y., Chen, J. H., Chen, S. Q., and Chen, F. H.: A climatological
537 northern boundary index for the East Asian summer monsoon and its interannual
538 variability, Sci. China Earth Sci., 48(1), 93–101, doi:https://doi.org/10.1007/s11430-017-
539 9122-x, 2018.
540 Cook, E. R.: A time series analysis approach to tree ring standardization (dendrochronology,
541 forestry, dendroclimatology, autoregressive process), Ph.D. thesis, The University of
542 Arizona, 1985.
543 Ding, A. J., Xiao, S. C., Peng, X. M., and Tian, Q. Y.: Shrub-ring reconstruction of precipitation
544 in the southeast of Tengger Desert, northwest China and its relationship with dust storm
545 events, Dendrochronologia, 126426, doi:https://doi.org/10.1016/j.dendro.2025.126426,
546 2025.
547 Ding, A. J., Xiao, S. C., Tian, Q. Y., and Han, C.: Correcting eccentric growth rings using basal
548 area increment: a case study for a desert shrub in Northwestern China, Tree-Ring Res.,
549 77(1), 1–9, doi:https://doi.org/10.3959/TRR2020-4, 2021.
550 Fang, K. Y., Gou, X. H., Chen, F. H., D'arrigo, R., and Li, J. B.: Tree-ring based drought
551 reconstruction for the Guiqing Mountain (China): linkages to the Indian and Pacific
552 Oceans, Int. J. Climatol., 30(8), 1137–1145, doi:https://doi.org/10.1002/joc.1974, 2010.
553 Fang, K. Y., Gou, X. H., Chen, F. H., Yang, M. X., Li, J. B., He, M. S., Zhang, Y., Tian, Q. H.,
554 and Peng, J. F.: Drought variations in the eastern part of northwest China over the past two
555 centuries: evidence from tree rings, Clim. Res., 38(2), 129–135,
556 doi:https://doi.org/10.3354/cr00781, 2009.
557 Feng, W., Wang, K. L., and Jiang, H.: Influences of westerly wind interannual change on water
558 vapor transport over northwest China summer, Plateau Meteorology, 23(2), 271–27, 2004.

https://doi.org/10.5194/egusphere-2026-2026
Preprint. Discussion started: 27 April 2026

559 Gou, X. H., Deng, Y., Gao, L. L., Chen, F. H., Cook, E., Yang, M. X., and Zhang, F.: Millennium
560 tree-ring reconstruction of drought variability in the eastern Qilian Mountains, northwest
561 China, Clim. Dyn., 45(7), 1761–1770, doi:https://doi.org/10.1007/s00382-014-2431-y,
562 2015a.
563 Gou, X. H., Gao, L. L., Deng, Y., Chen, F. H., Yang, M. X., and Still, C.: An 850-year tree-ring-
564 based reconstruction of drought history in the western Qilian Mountains of northwestern
565 China, Int. J. Climatol., 35(11), 3308–3319, doi:https://doi.org/10.1002/joc.4208, 2015b.
566 Guo, J. N., Xie, X. A., and Wang, A. Q.: A comparative study on the relationship between Asian
567 westerly jet position and summer precipitation in mid-latitude regions of East Asia and
568 Central Asia, J. Earth Sci. Environ., 16(01), 53–65,
569 doi:https://doi.org/10.7515/JEE222089, 2025.
570 Holmes, R. L.: Computer-assisted quality control in tree-ring dating and measurement, 1983.
571 Hu, H. R., and Qian, W. H.: Confirmation of the northern edge of the East Asian summer
572 monsoon, Prog. Nat. Sci., 17(1), 57–65, 2007.
573 Kang, S. Y., and Yang, B.: Precipitation variability at the northern fringe of the Asian summer
574 monsoon in Northern China and its possible mechanism over the past 530 years, Quat.
575 Sci., 35(5), 1185–1193, doi:https://doi.org/10.11928/j.issn.1001-7410.2015.05.14, 2015.
576 Li, D. L., Shao, P. C., and Wang, H.: The position variations of the north boundary of East Asia
577 subtropical summer monsoon in 1951–2009, Journal of Desert Research, 33(5), 1511,
578 2013.
579 Li, G. Q., Wang, X. Y., Zhang, X. J., Yan, Z. F., Liu, Y. L., Yang, H., Wang, Y. X., Jonell, T. N.,
580 Qian, J. K., Gou, S. Y., et al.: Westerlies-Monsoon interaction drives out-of-phase
581 precipitation and asynchronous lake level changes between Central and East Asia over the
582 last millennium, Catena, 218, 106568, doi:https://doi.org/10.1016/j.catena.2022.106568,
583 2022.
584 Li, J. L., Li, Z. R., Yang, J. C., Shi, Y. Z., and Fu, J.: Analyses on spatial distribution and
585 temporal variation of atmosphere water vapor over northwest China in summer of later 10
586 years, Plateau Meteorology, 31(6), 1574–1581, 2012.

https://doi.org/10.5194/egusphere-2026-2026
Preprint. Discussion started: 27 April 2026

587 Li, J. P., and Zeng, Q. C.: A new monsoon index, its interannual variability and relation with
588 monsoon precipitation, Clim. Environ. Res., 10(3), 351–365,
589 doi:https://doi.org/10.3878/j.issn.1006-9585.2005.03.09, 2005.
590 Li, S., Liu, X. W., and Sun, W.: Study of influence of rain shadow region on srudy
591 desertification in West of Hainan island based on wind tunnel experiments, Journal of
592 desert research, 26(2), 165–171, 2006.
593 Li, W. L., Wang, K. L., Fu, S. M., and Jiang, H.: The interrelationship between regional westerly
594 index and the water vapor budget in northwest China, Journal of Glaciology and
595 Geocryology, 30(1), 28–34, 2008.
596 Li, X., and Liu, X. D.: Relation of spring dust-storm activities in northern China and changes
597 of upper westerlies, Plateau Meteorology, 34(5), 1292–1300,
598 doi:https://doi.org/10.7522/j.issn.1000-0534.2014.00067, 2015.
599 Li, Y.: The pollen records from lake sediments and climate & lake model in the Marginal area
600 of Asian monsoon, Ph.D. thesis, Lanzhou University, Lanzhou, China, 2009.
601 Liang, E. Y., Liu, X. H., Yuan, Y. J., Qin, N. S., Fang, X. Q., Huang, L., Zhu, H. F., Wang, L.,
602 and Shao, X. M.: The 1920s drought recorded by tree rings and historical documents in
603 the semi-arid and arid areas of northern China, Clim. Change, 79(3), 403–432,
604 doi:https://doi.org/10.1007/s10584-006-9082-x, 2006.
605 Liu, W. C., Zhang, Q., and Fu, C.: Variation characteristics of precipitation and its affecting
606 factors in northwest China over the past 55 years, Plateau Meteorology, 36(6), 1533–1545,
607 2017.
608 Liu, Y., and Cai, Q. F.: The East Asia summer monsoon precipitation variations since AD 1840,
609 a case study of the tree-ring records from China and North Korean, Sci. China Earth Sci.,
610 33(6), 543–549, 2003.
611 Liu, Y., Cai, Q. F., Liu, W. G., Yang, Y. K., Sun, J. Y., Song, H. M., and Li, X. X.: Monsoon
612 precipitation variation recorded by tree-ring δ18O in arid Northwest China since AD 1878,
613 Chem. Geol., 252(1–2), 56–61, doi:https://doi.org/10.1016/j.chemgeo.2008.01.024, 2008.
614 Liu, Y., Cai, Q. F., Ma, L. M., and An, Z. S.: Tree ring precipitation records from Baotou and
615 the East Asia summer monsoon variations for the last 254 years, Earth Sci. Front., 8(1),
616 91–97, 2001.

https://doi.org/10.5194/egusphere-2026-2026
Preprint. Discussion started: 27 April 2026

617 Liu, Y., Sun, C. F., Li, Q., and Cai, Q. F.: A Picea crassifolia tree-ring width-based temperature
618 reconstruction for the Mt. Dongda region, Northwest China, and its relationship to large-
619 scale climate forcing, PLoS One, 11(8), e0160963,
620 doi:https://doi.org/10.1371/journal.pone.0160963, 2016.
621 Liu, Y. Z., Wu, C. Q., Jia, R., and Huang, J. P.: An overview of the influence of atmospheric
622 circulation on the climate in arid and semi-arid region of Central and East Asia, Sci. China
623 Earth Sci., 48(9), 1141–1152, doi:https://doi.org/10.1007/s11430-017-9202-1, 2018.
624 Luo, Y., Xu, C. C., Li, Z. Y., Li, L., Wang, Q., and Zhang, Q. Y.: Synergistic enhancement of
625 Asian monsoons to westerlies intensifies the drying trend of arid Central Asia over the last
626 20 years, Gondwana Res., 149, 337-350, doi:https://doi.org/10.1016/j.gr.2025.08.021,
627 2026.
628 Ma, M. J., Pu, Z. X., Wang, S. O., and Zhang, Q.: Characteristics and numerical simulations of
629 extremely large atmospheric boundary-layer heights over an arid region in north-west
630 China, Bound.-Layer Meteor., 140(1), 163–176, doi:https://doi.org/10.1007/s10546-011-
631 9608-2, 2011.
632 Mcgowan, A. H., and Andrew, P. S.: Regional and local scale characteristics of Foehn wind
633 events over the South Island of New Zealand, Meteorology And Atmospheric Physics, 58,
634 151-164, doi:https://doi.org/10.1007/BF01027562, 1994.
635 Ou, T. H., and Qian, W. H.: Vegetation variations along the monsoon boundary zone in East
636 Asia, Chinese Journal of Geophysics - Chinese edition, 49(3), 627–636, 2006.
637 Peng, X. M., Zhang, B. W., Wang, W. S., Ding, A. J., and Xiao, S. C.: Different drought indices
638 showed different variations and applicability to dendrochronological studies,
639 Dendrochronologia, 84, 126179, doi:https://doi.org/10.1016/j.dendro.2024.126179, 2024.
640 Qu, W. J., Zhang, X. Y., Wang, D., Shen, Z. X., Mei, F. M., Cheng, Y., and Yan, L. W.: The
641 important significance of westerly wind study, Marine Geology & Quaternary Geology,
642 24(1), 125–132, 2004.
643 Ren, Y., Xiao, S. C., Peng, X. M., Ding, A.J., Tian, Q. Y., Wang, J.K.: Shrub dendrochronology
644 reveals the last 150 years of spatiotemporal patterns of desertification in the Tengger
645 Desert. Catena 264 (2026) 109844. https://doi.org/10.1016/j.catena.2026.109844

https://doi.org/10.5194/egusphere-2026-2026
Preprint. Discussion started: 27 April 2026

646 Sun, D. H., An, Z. S., Su, R. X., Lu, H. Y., and Sun, Y. B.: The dust deposition records of the
647 evaluation of Asia monsoon and Westerly circulation in north China in the last 2.6 Ma, Sci.
648 China Earth Sci., 33(6), 497–504, doi:https://doi.org/10.1007/s11430-025-1596-y, 2003.
649 Tang, X., Qian, W. H., and Liang, P.: Climatic features of boundary belt for East Asian summer
650 monsoon, Plateau Meteorology, 25(3), 375–381, 2006a.
651 Tang, X., Sun, G. W., and Qian, W. H.: Study on the north edge of the Asia Summer Monsoon,
652 Atmosphere Press, 2006b.
653 Wang, J. L., Yang, B., Ljungqvist, F. C., Luterbacher, J., Osborn, T. J., Briffa, K. R., and Zorita,
654 E.: Internal and external forcing of multidecadal Atlantic climate variability over the past
655 1,200 years, Nat. Geosci., 10(7), 512–517, doi:https://doi.org/10.1038/ngeo2962, 2017.
656 Wang, J. S.: Study on regional climate response to global warming in the arid central-east Asia
657 over the past 100a, Ph.D. thesis, Lanzhou University, Lanzhou, 2006.
658 Wang, K. L., Jiang, H., and Zhao, H. Y.: Atmospheric water vapor transport from westerly and
659 monsoon over the Northwest China, Advances in Water Science, 16(3), 432–438,
660 doi:https://doi.org/10.14042/j.cnki.32.1309.2005.03.021 2005.
661 Xiao, S. C., Chen, X. H., and Ding, A. J.: Study process of climate changes, environment
662 evolution and its driving mechanism in the last two centuries in the Alxa Desert, Journal
663 of Desert Research, 37(6), 1102-1110, doi:https://doi.org/10.7522/j.issn.1000-
664 694X.2017.00002, 2017.
665 Xiao, S. C., Peng, X. M., Tian, Q. Y., Ding, A. J., Xie, J. L., and Su, J. R.: Interaction between
666 the East Asian summer monsoon and westerlies as shown by tree-ring records, Clim. Past.,
667 20(7), 1687–1701, doi:https://doi.org/10.5194/cp-20-1687-2024, 2024a.
668 Xiao, S. C., Su, J. R., Peng, X. M., and Tian, Q. Y.: Review on the study of monsoon-westerly
669 interaction in the inland arid none of northwestern China, Plateau Meteorology, 43(6),
670 1355–1363, doi:https://doi.org/10.7522/j.issn.1000-0534.2024.00028, 2024b.
671 Xiao, S. C., Xiao, H. L., Dong, Z. B., and Peng, X. M.: Dry/wet variation recorded by shrub
672 tree-rings in the central Badain Jaran Desert of northwestern China, J. Arid Environ., 87,
673 85–94, doi:https://doi.org/10.1016/j.jaridenv.2012.06.013, 2012.
674 Xiao, S. C., Yan, C. Z., Tian, Y. Z., Si, J. H., Ding, A. J., Chen, X. H., Han, C., and Teng, Z. Y.:
675 Regionalization for desertification control and countermeasures in the Alxa Plateau, China,

https://doi.org/10.5194/egusphere-2026-2026
Preprint. Discussion started: 27 April 2026

676 Journal of Desert Research, 39(5), 182–19, doi:https://doi.org/10.7522/j.issn.1000-
677 694X.2019.00068, 2019.
678 Xu, Y., and Qian, W. H.: Research on East Asia monsoon： a review, Acta Geographica Sinica,
679 (z1), 138–146, 2003.
680 Yuan, L.: Hazards history in northwestern China, Gansu people's press, Lanzhou, China, 1994.
681 Zhang, Q., Yang, J. H., Wang, P. L., Yu, H. P., Yue, P., Liu, X. Y., Lin, J. J., Duan, X. Y., Zhu,
682 B., and Yan, X. Y.: Progress and prospect on climate warming and humidification in
683 Northwest China, Chin. Sci. Bull., 68(14), 1814–1828, doi:https://doi.org/10.1360/TB-
684 2022-0643, 2023.
685 Zhang, Q. Y., Tao, S. Y., and Chen, L. T.: The inter-annual variability of east asian summer
686 monsoon indices and its association with the pattern of general circulation over east Asia,
687 Acta Meteorol. Sin., (05), 559–56, 2003.
688 Zhong, H. L., and Li, D. L.: Relationship between sand-dust storm in northern China in April
689 and westerly circulation, Plateau Meteorology, 24(1), 104–111, 2005.